[CANCER RESEARCH 60, 5134–5142, September 15, 2000]

CD99 Engagement: An Effective Therapeutic Strategy for Ewing Tumors[1]

Katia Scotlandi,[2] Nicola Baldini, Vanessa Cerisano, Maria Cristina Manara, Stefania Benini, Massimo Serra, Pier-Luigi Lollini, Patrizia Nanni, Giordano Nicoletti, Ghislaine Bernard, Alain Bernard, and Piero Picci

Laboratorio di Ricerca Oncologica, Istituti Ortopedici Rizzoli, Bologna, 40136 Italy [K. S., N. B., V. C., M. C. M., S. B., M. S., P. P.]; Istituto di Cancerologia, Università di Bologna, 40126 Bologna, Italy [P. N., P-L. L.]; IST, Istituto Nazionale per la Ricerca sul Cancro-Genova, Unità Satellite di Biotecnologie, 40126 Bologna, Italy [G. N.]; and Unité Institut National de la Santé et de la Recherche Médicale 343, Hôspital de l'Archet, Nice Cedex 3, France [G. B., A. B.]

ABSTRACT

CD99 is a M_r 32,000 transmembrane molecule that shows a high level of expression on cells of the hemopoietic system as well as on Ewing tumor cells. Within the hematopoietic system, CD99 has been implicated in cell adhesion and cell death, participating in this way in the differentiation of T-cell precursors. In this study, we demonstrate that engagement of CD99 significantly inhibits the *in vitro* and *in vivo* growth ability of Ewing tumor cells by delivering an apoptotic stimulus and reducing the malignant potential of these cells. Moreover, we show that anti-CD99 monoclonal antibodies may be advantageously used in association with conventional anticancer agents. These results provide a novel entry site for therapeutic intervention, which may have application in the care of patients with Ewing tumor, and warrant additional studies to clarify the molecular mechanisms activated by CD99 engagement.

INTRODUCTION

The EFT[3] comprises ES, Askin's tumor of the thoracic wall, and peripheral PNET, all these lesions being small round cell malignancies of bone and soft tissues that show an extremely aggressive clinical course (1). Besides a similar histological picture, these neoplasms share the presence of an *EWS-ets* gene rearrangement (2) as well as the uniform expression of the *CD99/MIC2* gene at high levels (3, 4) and are currently defined along a limited gradient of neural differentiation, with the poorly differentiated ES at one end and the most differentiated PNET at the other. Although the chance of survival of nonmetastatic EFT patients has been significantly improved by the adoption of multidrug chemotherapy in addition to surgery and/or radiation therapy (5–7), the cure rate remains still as low as 20% in high-risk groups (8, 9), including patients with primitive lesions in the axial skeleton. Moreover, recent clinical studies have indicated that the survival rate of EFT patients has reached a plateau phase and, very likely, the highest levels achievable by conventional multimodal therapy (6). The identification of new targets for innovative therapeutic approaches are, therefore, strongly needed for this tumor. Targeted therapies based on a thorough understanding of the biological processes specifically involved in the pathogenesis and progression of a single neoplasm are now considered as a promising basis for ideal cancer management. These strategies may either specifically target neoplastic proliferation or induce cell death or terminal differentiation of tumor cells. We have recently proposed targeting of insulin-like growth factor receptor I as a possible strategy to deregulate EFT tumor growth (10, 11). Here, we identify in the engagement of CD99, another entry site for therapeutic intervention in EFT. Whereas the blockage of insulin-like growth factor receptor I resulted in a cytostatic effect, the engagement of CD99 appears to be able to induce massive apoptosis and to reduce the malignant potential of EFT cells, therefore representing a more promising target for a tailored therapy of these neoplasms.

CD99 is an integral M_r 32,000 transmembrane glycoprotein encoded by the *MIC-2* gene, which is located to the pseudoautosomal regions of both human X and Y chromosomes, and shares no homology with any known protein, with the exception of the PBDX product, the function of which is unknown (12–14). CD99 is broadly distributed on many types of normal cells, with a particularly strong expression on cells of the T-cell lineage (15) and on EFT (3, 4). The expression density on T-lineage cells seems to be linked to the maturation of T lymphocytes. The high levels of expression on EFT cells are implicated as a diagnostic tool for the differential evaluation of small round cell tumor of childhood (3). The function of CD99 remains largely undefined. Within the hematopoietic system, CD99 has been implicated in cell-to-cell adhesion during hematopoietic differentiation (16, 17), apoptosis of immature thymocytes (18), and up-regulation of several transmembrane proteins (19, 20). More recently, a role for CD99 in the regulation of cell cycle and differentiation has been demonstrated (21, 22). In EFT, engagement of CD99 has been shown recently to have a functional role in inducing apoptosis (23). Therefore, given that death signal transduction via CD99 may also occur in EFT cells, we assessed the role of this antigen in regulating the cell growth ability and the malignant potential of EFT by the analysis of seven EFT cell lines, representative of the three different variants included in this group of neoplasms.

MATERIALS AND METHODS

Cell Lines. ES cell lines SK-ES-1, RD-ES, and SK-N-MC as well as the osteosarcoma cell line U-2 OS were obtained from the American Type Culture Collection (Rockville, MD). ES cell lines TC-71 and 6647 cell line were a generous gift from T. J. Triche (Childrens Hospital, Los Angeles, CA). PNET cell lines LAP-35 and IOR/EW4 were established previously at the Istituti Ortopedici Rizzoli (Bologna, Italy). The Jurkat T cell line was a kind gift of A. Bernard (Hôspital de L'Archet, Nice, France). Cells were routinely cultured in IMDM, supplemented with 100 units/ml penicillin, 100 μg/ml streptomycin (Life Technologies, Inc., Paisley, Scotland), and 10% inactivated FCS (Biological Industries, Kibbutz Beth Haemek, Israel). Cells were maintained at 37°C in a humidified 5% CO_2 atmosphere.

MAbs and Reagents. The anti-CD99 0662 MAb was produced in the Unité INSERM 343, Hopital de l' Archet, Nice, France and clusterized during the Human Leukocyte Differentiation Agents International Workshop in 1989 and 1993 (24). Anti-CD99 MAb (clone 013; Signet, Dedham, MA; Ref. 24), anti-Fas CD95 MAb (clone SM1/1; Bender MedSystems, Vienna, Austria), anti-BrdUrd MAb (Becton Dickinson, Milan, Italy) were obtained commercially. Doxorubicin, vincristin, and Hoechst 33258 were purchased from Sigma Chemical Co. (St. Louis, MO). Annexin V-FITC apoptosis detection kit was obtained from MBL (Medical & Biological Laboratories, Naka-ku Nagaya, Japan).

Analysis of Growth Features. To study the effects of anti-CD99 Mabs on the *in vitro* cell growth, cells were seeded in 24-well plates (cells/well: 250,000 for TC-71 and U-2 OS; 500,000 for SK-N-MC, SK-ES-1, 6647, RD-ES, LAP-35,IOR/EW4, and Jurkat) in IMDM plus 10% FCS. After 24 h, medium was changed with IMDM plus 10% FCS, with or without

Received 2/24/00; accepted 7/20/00.

The costs of publication of this article were defrayed in part by the payment of page charges. This article must therefore be hereby marked *advertisement* in accordance with 18 U.S.C. Section 1734 solely to indicate this fact.

[1] This work was supported by grants from the Associazione Italiana per la Ricerca sul Cancro, the Italian Ministry for University and Research, the Rizzoli Institute, and the Italian Ministry of Health (Ricerca Finalizzata).

[2] To whom requests for reprints should be addressed, at Laboratorio di Ricerca Oncologica, Istituti Ortopedici Rizzoli, Via di Barbiano, 1/10, 40136 Bologna, Italy. Fax: 39-051-6366-761; E-mail: katia.scotlandi@ior.it.

[3] The abbreviations used are: EFT, Ewing family of tumors; ES, Ewing's sarcoma; PNET, primitive neuroectodermal tumor; MAb, monoclonal antibody; BrdUrd, bromodeoxyuridine; IMDM, Iscove's Modified Dulbecco's Medium.

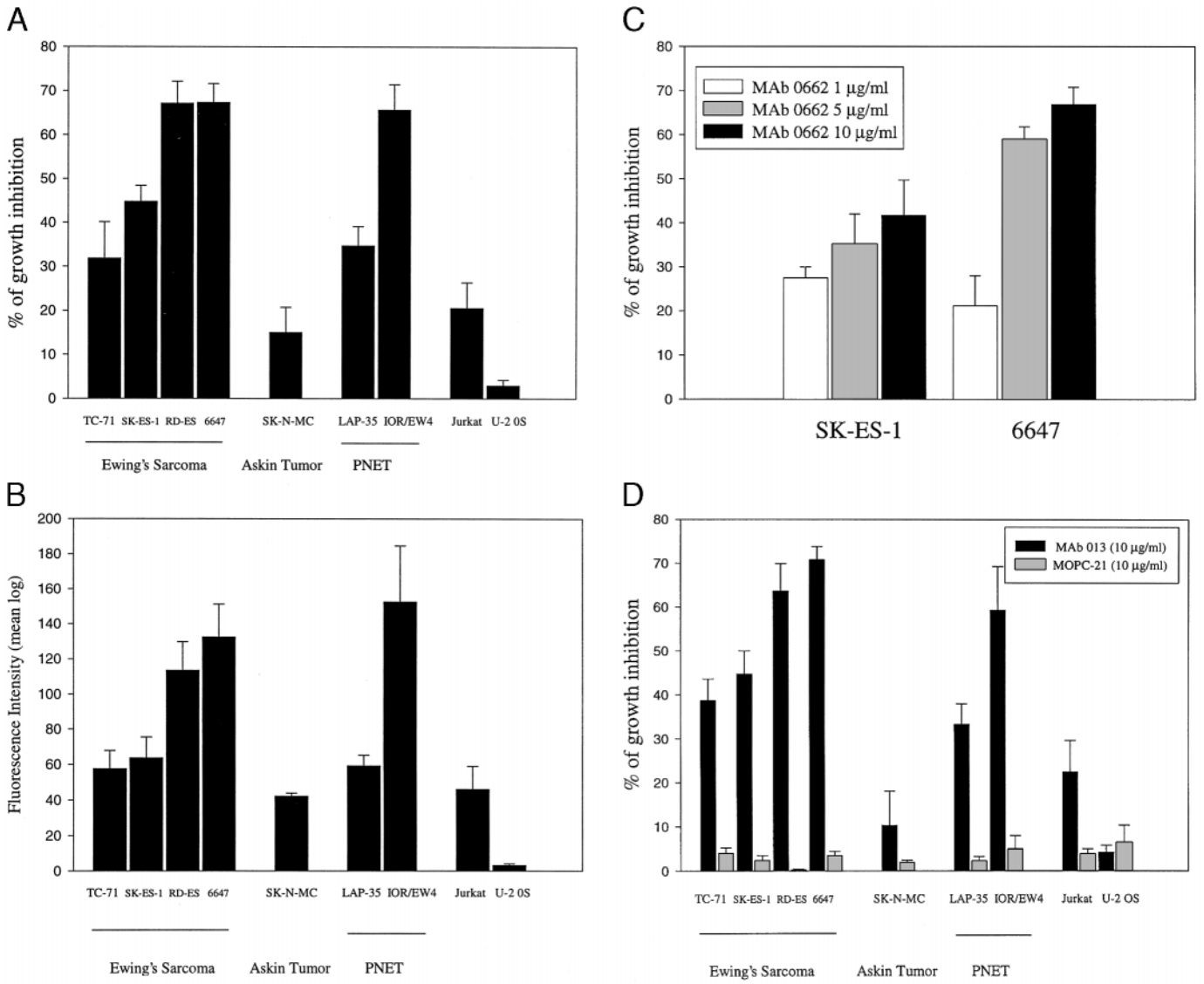

Fig. 1. Engagement of CD99 by anti-CD99 MAb induces a significant dose-dependent *in vitro* growth inhibition of EFT cells in relation to the level of expression of CD99 on the cell surface. *A*, inhibition of EFT cell growth after 24 h of *in vitro* treatment with the anti-CD99 0662 MAb (10 μg/ml). Results are expressed as the percentage of growth inhibition compared with controls. *B*, expression of CD99 in EFT cell lines as determined by flow cytometry. *C*, inhibition of EFT cell growth after 24 h of *in vitro* treatment with different doses of the anti-CD99 0662 MAb. Results are expressed as the percentage of growth inhibition compared with controls. *D*, inhibition of EFT cell growth after 24 h of *in vitro* treatment with 10 μg/ml of the anti-CD99 013 or MOPC-21 MAbs. Results are expressed as the percentage of growth inhibition compared with controls. *Bars*, SE.

(control) anti-CD99 Mabs (1–10 μg/ml). As an additional control, the isotype-matched control antibody MOPC-21 (Sigma) was also used (10 μg/ml). Cell growth was evaluated on harvested cultures by trypan blue vital cell count. A similar procedure was also used to analyze the effects of the anti-CD95 inducing apoptosis SM1/1 MAb in EFT cells. For the evaluation of BrdUrd labeling index, cells treated as described above were incubated with 10 μM BrdUrd (Sigma) for 1 h in a CO_2 atmosphere at 37°C. Harvested cells were fixed in 70% ethanol for 30 min. After DNA denaturation with 2 N HCl for 30 min at room temperature, cells were washed with 0.1 M $Na_2B_4O_7$ (pH 8.5). Cells (10^6) were then processed for indirect immunofluorescence staining, using anti-BrdUrd MAb diluted 1:4 as a primary antibody (Becton Dickinson), and analyzed by flow cytometry (FACScan; Becton Dickinson). The analysis of apoptotic cells was assessed by morphological evaluation, analysis of DNA content, and analysis of Annexin-positive cells. In particular, for morphological evaluation, cells were fixed in methanol:acetic acid (3:1) for 15 min and stained with 50 ng/ml Hoechst 33258. Cells with three or more chromatin fragments were considered apoptotic. For the analysis of DNA content, cells were fixed with cold 70% ethanol, treated with 0.5 mg/ml RNase, and stained with 25 μg/ml propidium iodide. The fraction of hypodiploid cells was estimated

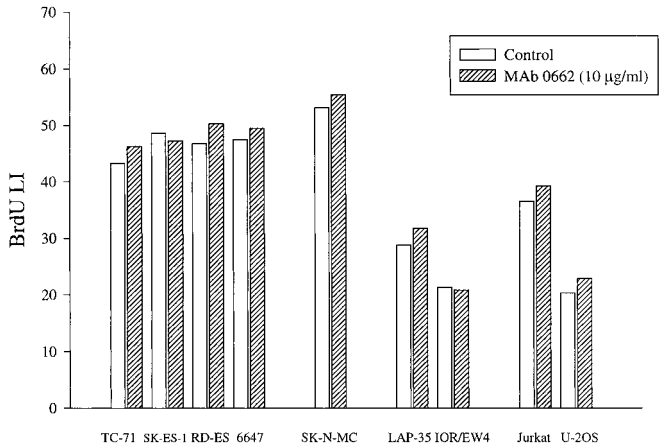

Fig. 2. Effects on the proliferative rate of EFT cell lines after 24-h treatment with anti-CD99 MAb. Results of individual experiments, representative of at least two different similar experiments, are expressed as the percentage of BrdUrd-positive cells (*BrdU LI*) as determined by flow cytometry.

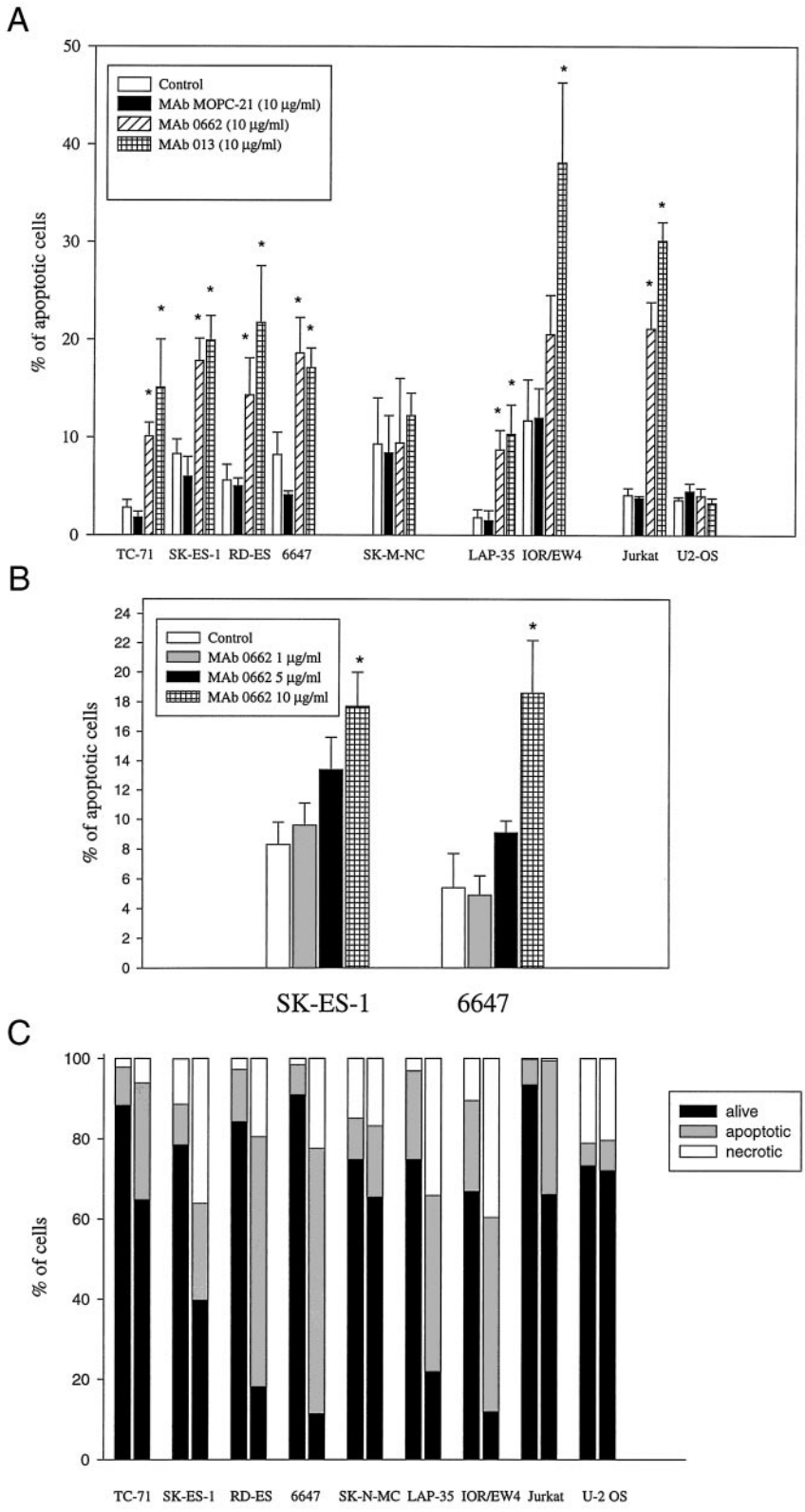

Fig. 3. CD99 MAbs induce apoptosis in EFT cells. *A*, histograms of cytofluorometric analysis of hypodiploid cells after 24 h of treatment with the anti-CD99 MAbs or the control MOPC-21 MAb. *, $P < 0.05$, paired Student's *t* test. *B*, cytofluorometric analysis of hypodiploid cells after 24-h of treatment with different doses of anti-CD99 0662 MAb. *, $P < 0.05$, paired Student's *t* test. *Bars*, SE. *C*, cytofluorometric analysis of apoptotic EFT cells by Annexin V and propidium iodide after 24 h of treatment with 10 μg/ml of the anti-CD99 013 MAb. The simultaneous application of propidium iodide as a DNA stain, which is used for dye exclusion tests, allows the discrimination of necrotic cells from the Annexin V positively stained cells. Results of individual experiments, representative of different similar experiments using 013 or 0662 MAb, are shown. For each cell line, the *left* and *right* histograms indicate results obtained for control and treated cells, respectively. *D*, time course of apoptosis induced by 10 μg/ml of 013 MAb as measured by Annexin V fluorescence staining. *E*, representative spectrum of cytofluorometric analysis of hypodiploid cells (on the *left*) and apoptotic cells by Annexin V and propidium iodide (on the *right*) after 24-h treatment of RD-ES cells with 10 μg/ml of the anti-CD99 013 MAb.

by flow cytometry. Detection and quantification of apoptotic cells was also obtained by the flow cytometric analysis of annexin-V-labeled cells. This test was performed according to the manufacturer's instructions. Annexin V is a Ca^{2+}-dependent phospholipid protein with high affinity for phosphatidylserine. This protein can hence be used as a sensitive probe for phosphatidylserine exposure upon the outer layer of the cell membrane and is therefore suited to detect apoptotic cells. Because necrotic cells also expose phosphatidylserine according to the loss of membrane integrity, the simultaneous application of propidium iodide as a DNA stain is required to discriminate necrotic from apoptotic cells.

CD99 and Fas/CD95 Expression. The expression of CD99 and of CD95 at the cell surface was analyzed by indirect immunofluorescence and flow cytometry using the 013 MAb (diluted 1:80) and the SM1/1 MAb (diluted 1:50), respectively.

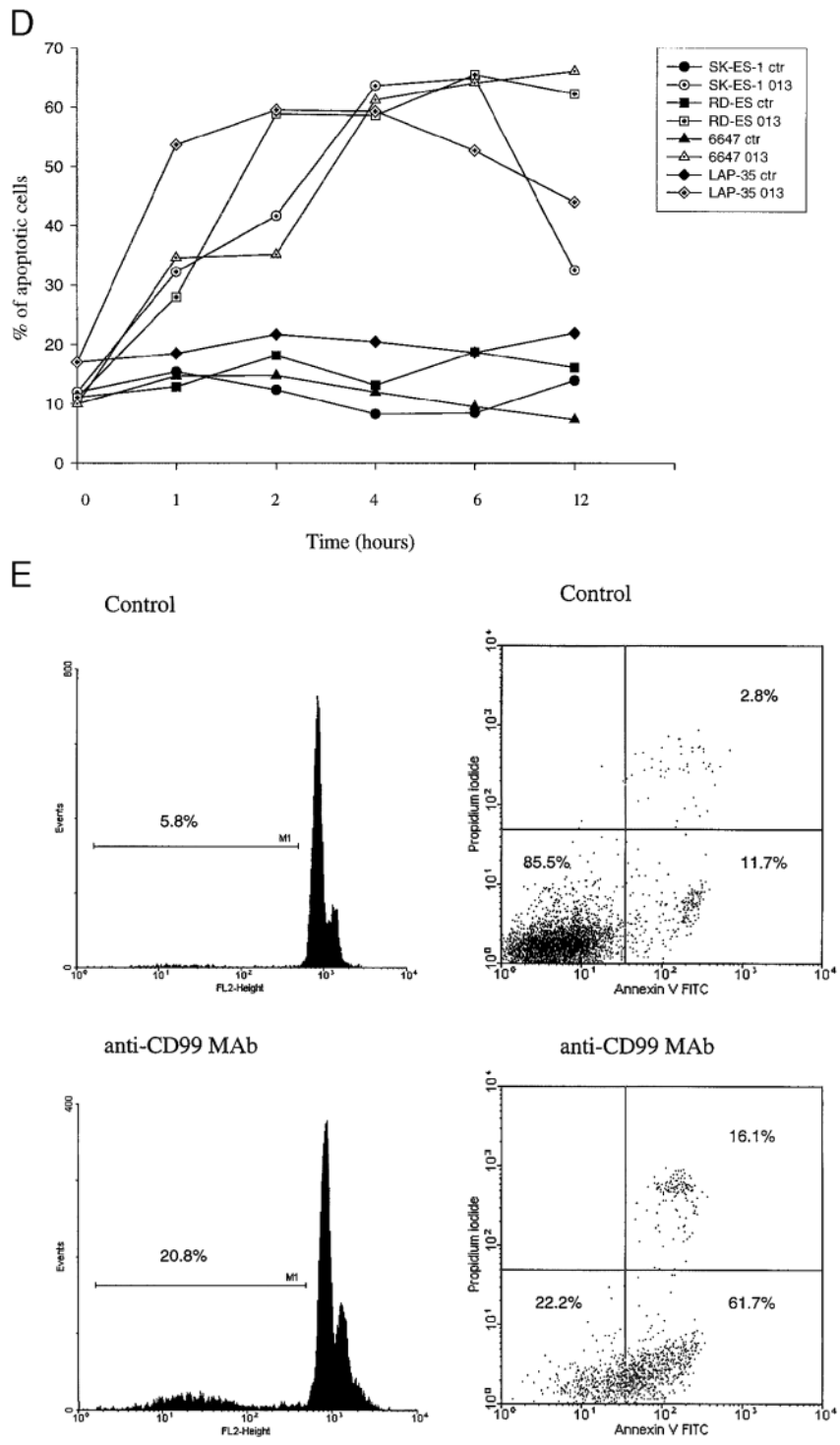

Fig. 3. (Continued).

Homotypic Adhesion Assay. Homotypic adhesion assay was performed as described previously (25). Briefly, 2 ml of a 10^7 cells/ml unicellular suspension were incubated at 37°C for 15–60 min. At the end of the incubation, cells were resuspended with a large-bore Pasteur pipette. Homotypic adhesion was then evaluated microscopically by counting single cells at the end of the procedure.

Soft-Agar Assay. Anchorage-independent growth was determined in 0.33% agarose (SeaPlaque; FMC BioProducts, Rockland, ME) with a 0.5% agarose underlay. Cell suspensions were plated in a semisolid medium (IMDM plus 10% FCS containing 0.33% agarose) with or without anti-CD99 (10 μg/ml; cells/dish, 1000–3300). The control antibody MOPC-21(10 μg/ml) was also used as an additional control. Dishes were incubated at 37°C in a humidified atmosphere containing 5% CO_2, and colonies were counted after 7 days.

***In Vivo* Treatment with Anti-CD99 0662 MAb.** Female athymic Crl/*nu/nu* (CD-1) BR mice (Charles River Italia, Como, Italy), 4–5 weeks of age, were used. Tumorigenicity was determined after s.c. injection of 5×10^6 6647 cells. Twenty-four h after cell injection, the animals were randomized into control and treated groups. In the latter group, each mouse received s.c. injection of 0662 MAb (40 μg/injection) in proximity of the tumor three times a week, starting from the day after tumor implantation. Control mice received s.c. injection of PBS or the class-matched IgG MOPC-21 (40 μg/injection; additional control group for 0662 MAb treatment). The treatment period consisted of eight injections. Tumor growth was assessed once weekly by measuring tumor volume, calculated as $\pi/6 \times [\sqrt{}(ab)]^3$, where a and b are the two major diameters. For ethical reasons, mice were sacrificed and necropsied

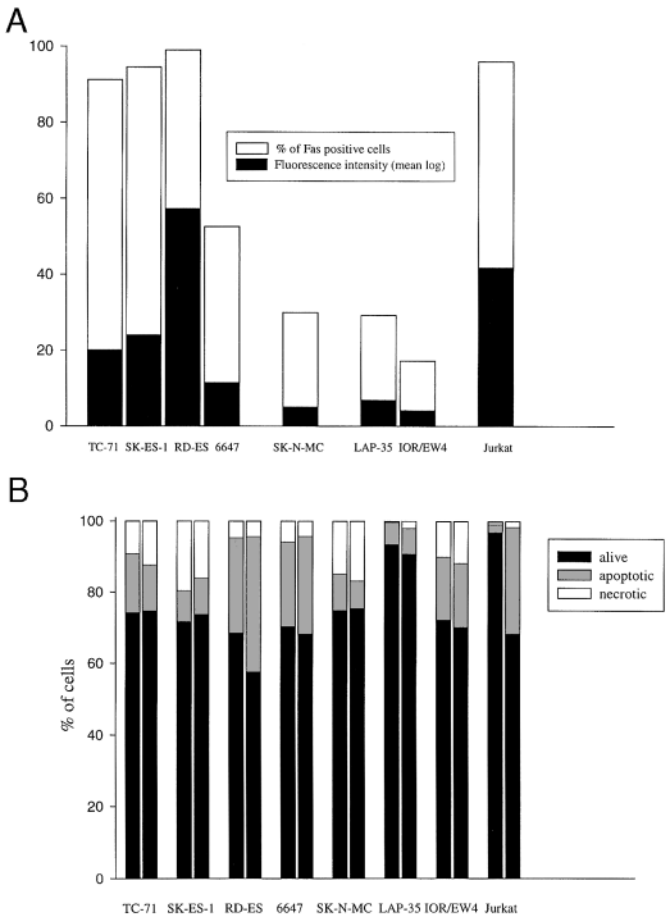

Fig. 4. Fas/CD95 MAb fails to induce apoptosis in EFT cell lines. *A*, expression of Fas/CD95 in EFT cell lines as determined by flow cytometry. *B*, cytofluorometric analysis of apoptosis in EFT cells by Annexin V and propidium iodide staining after 24 h of treatment with anti-CD95 SM1/1 MAb (1 μg/ml). Results of individual experiments, representative of at least two different similar experiments, are shown. For each cell line, the *left* and *right* histograms indicate results obtained for control and treated cells, respectively.

when the mean tumor volume was 5 ml. Tumors were fixed in 10% buffered formaldehyde for at least 48 h and processed for histological examination. Sections of the tumors were stained with H&E and analyzed microscopically.

Cytotoxic Effects of Doxorubicin or Vincristin in Association with Anti-CD99 0662 MAb. Cells (100,000) were seeded in 24-well plates in IMDM plus 10% FCS, and treatment started the next day. Cells were pretreated with or without (control) 10 μg/ml of 0662 MAb and, after 12 h, varying concentrations of doxorubicin (range, 10 pg/ml to 10 ng/ml) or vincristin (range, 100 pg/ml to10 ng/ml) were added to appropriate wells. After 72 h, cell growth was evaluated on harvested cultures by trypan blue vital cell count.

Statistical Analysis. Differences among means were analyzed using Student's *t* test. Fisher's exact test was used for frequency data. Correlations were analyzed using Spearman's test. The analysis of drug combination effects was performed by using the fractional product method.

RESULTS

Engagement of CD99 Induces *in Vitro* Growth Inhibition Attributable to an Apoptotic Stimulus. We found that ligation of CD99 with the anti-CD99 0662 monoclonal antibody (MAb; Ref. 24) resulted in a significant *in vitro* growth inhibition of EFT cells (Fig. 1*a*). This effect was observed after 24-h of *in vitro* treatment and appeared to be strictly related to the level of expression of CD99 (Fig. 1*b*; $r = 0.95$, $P < 0.001$, Spearman's test). Jurkat T cells and U-2 OS osteosarcoma cells were included in the analysis as positive (18) and negative controls, respectively. The observed growth-inhibitory effect was dependent on the concentration of 0662 MAb (Fig. 1*c*) and appeared to be specifically attributable to CD99 ligation because an equivalent amount of an isotype control MAb had no effect on the growth of EFT cells (Fig. 1*d*). The specificity of CD99 signaling was further demonstrated using an additional MAb (clone 013; Ref. 24) directed against a different epitope of CD99. As shown in Fig. 1*d*, 24-h treatment of EFT cells with 013 MAb similarly inhibited EFT cell growth at the dose of 10 μg/ml. The growth inhibition induced by CD99 engagement was not attributable to a reduction in the proliferative rate, as indicated by BrdUrd labeling (Fig. 2), but rather to a significant induction of apoptosis. Anti-CD99 MAbs (either 0662 or 013) significantly induced a dose-dependent programmed cell death in all of the EFT cell lines, with the exception of SK-N-MC cells. Fig. 3, *a* and *b*, shows the percentage of hypodiploid EFT cells, following 24-h of *in vitro* treatment with anti-CD99 MAbs. Again, the ability of CD99 molecules to trigger a death signal appeared to be related to the levels of expression of this antigen in EFT cells ($r = 0.67$, $P = 0.05$, Spearman's test). In agreement with previous results (18), the induction of apoptosis was also observed in Jurkat cells (Fig. 3*a*). U-2 OS cells, which do not express CD99, failed to present apoptosis after anti-CD99 MAb treatment. CD99-induced apoptosis in EFT cells was further confirmed by using a fluorescent conjugate of Annexin V. This protein has a strong affinity for the membrane phospholipid phosphatidylserine (26, 27), a molecule that has been reported to be translocated from the inner face of the plasma membrane to the cell surface soon after the beginning of the apoptotic process (28). Similarly to the analysis of hypodiploid nuclei, the Annexin assay revealed a significant increase in the percentage of apoptotic cells in all of the EFT cell lines, with the exception of SK-N-MC cells (Fig. 3*c*). A time course analysis of the induction of apoptosis in EFT cell lines showed that cell death was clearly observed in EFT cells within 1–2 h after anti-CD99 treatment (Fig. 3*d*). Maximal apoptosis was evident within 4–6 h. Fig. 3*e* shows a representative

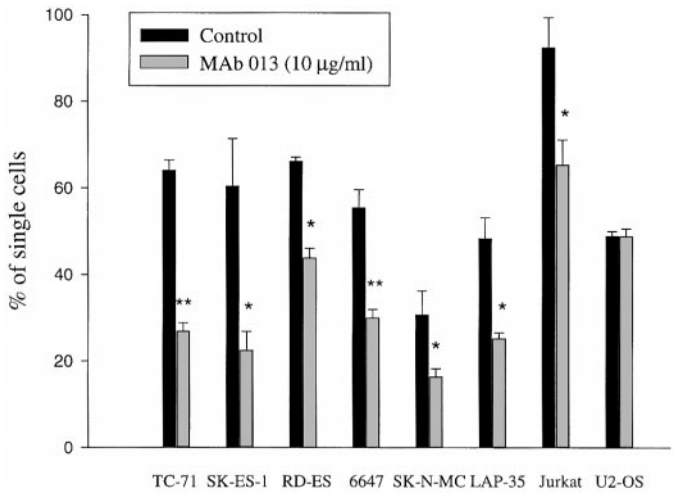

Fig. 5. CD99 engagement by specific MAbs induces a higher homotypic adhesion of EFT cells. The proportion of cells remaining single at the end of the experiment is shown. Each *column* represents the mean of four independent experiments; *bars*, SE. *, $P < 0.05$, paired Student's *t* test. **, $P < 0.001$, paired Student's *t* test.

Table 1 *Effects on colony formation in soft agar by anti-CD99 MAb treatment*

	Control[a]	MOPC-21 10 μg/ml	anti-CD99 (013) 10 μg/ml
6647	1573 ± 125	1618 ± 202	9 ± 3[b]
SK-ES-1	580 ± 44	616 ± 183	2 ± 2[b]

[a] Cells (3300) were plated in 0.33% agarose with medium plus 10% FCS with or without (control) MAbs, and colonies were counted after 7 days. Data are expressed as means of triplicate plates ± SE.

[b] $P < 0.001$, Student's *t* test.

spectrum of cytofluorometric analysis of apoptotic cells in anti-CD99-treated and control EFT cells. In agreement with findings observed by Bernard *et al.* (18) and by Sohn *et al.* (23), apoptosis of EFT cells after CD99 engagement was not accompanied by DNA fragmentation (not shown). Although all of the EFT cell lines examined here expressed variable levels of the death receptor Fas/CD95 on their surface (Fig. 4*a*), no significant induction of apoptosis was observed after treatment of these cells with the Fas-inducing MAb SM1/1 (Fig. 4*b*). These findings indirectly support the observations of Bernard *et al.* (18) in Jurkat cells and confirm that CD99-mediated apoptosis is independent from Fas/CD95 intracellular signaling cascade.

Effect of CD99 on Homotypic Aggregation. CD99 appears to regulate adhesion properties of T cells, in particular the induction of homotypic adhesion in immature, double-positive ($CD4^+CD8^+$) thymocytes (16, 17). Similarly, we found that the treatment of EFT cells with anti-CD99 MAbs (0662 or 013) resulted in a significant induction of the homotypic adhesion potential of these cells, as indicated by the formation of cell clumps in a homotypic adhesion assay. Fig. 5 shows that the proportion of EFT cells remaining single at the end of the assay was significantly lower after CD99 engagement.

CD99 Engagement and Malignancy of EFT Cells. Triggering of CD99 was also able to abolish the ability of EFT cells to grow in a semisolid medium. In fact, treatment with 013 MAb induced a significant inhibition in the number of colonies of 6647 and SK-ES-1 cells (Table 1), indicating that engagement of this molecule is also able to inhibit the malignant potential of EFT cells. The loss of malignancy was confirmed by an *in vivo* study. To analyze the effects of CD99 engagement on the *in vivo* growth of EFT cells, randomized athymic mice, s.c. injected with 6647 cells, were locally treated with 0662 MAb (40 μg/injection), MOPC-21 (40 μg/injection), or PBS. Treatment started 24 h after the injection of 5×10^6 cells, a dose that is able to produce tumors in all untreated animals. The treatment period consisted of eight injections in the first 2 weeks. At the end of the treatment, the number of tumor-free mice was 3 of 5 (60%) in the anti-CD99 group, 0 of 4 in the MOPC-21 group, and 0 of 10 in the PBS group ($P = 0.02$, Fisher's test, between the anti-CD99 group and PBS group). Moreover, by considering the mice in which tumors developed during or after the treatment period, a growth-inhibitory effect of anti-CD99 treatment was generally observed, as shown by the *in vivo* growth curve of 6647 cells in individual mice (Fig. 6). Histological examination of tumor specimens showed a higher amount of apoptotic cells in anti-CD99 MAb-treated animals compared with controls (Fig. 7).

Combination Treatments with Conventional Cytotoxic Drugs. To further analyze the therapeutic potential of CD99 targeting, we investigated the effects on the *in vitro* growth of EFT cells after combination therapy with MAb plus conventional anticancer agents. In particular, we analyzed whether anti-CD99 MAb and doxorubicin or vincristin, two leader drugs in the treatment of EFT patients (6), have competitive, additive, or synergistic action to inhibit the growth of EFT cells. To closely mimic the clinical situation, a sequential treatment was designed. EFT cells were first treated with 10 μg/ml 0662 MAb for 12 h and then with different doses of doxorubicin or vincristin. An additive growth suppression effect attributable to the combination treatment was observed, resulting in an enhancement of the antitumor activity of doxorubicin or vincristin by pretreating cells with anti-CD99 MAb 0662 (Fig. 8). The IC_{50}s showed a 153- and 4-fold decrease for doxorubicin and vincristin in 6647 cells and a 59- and 2-fold decrease in SK-ES-1 cells, respectively.

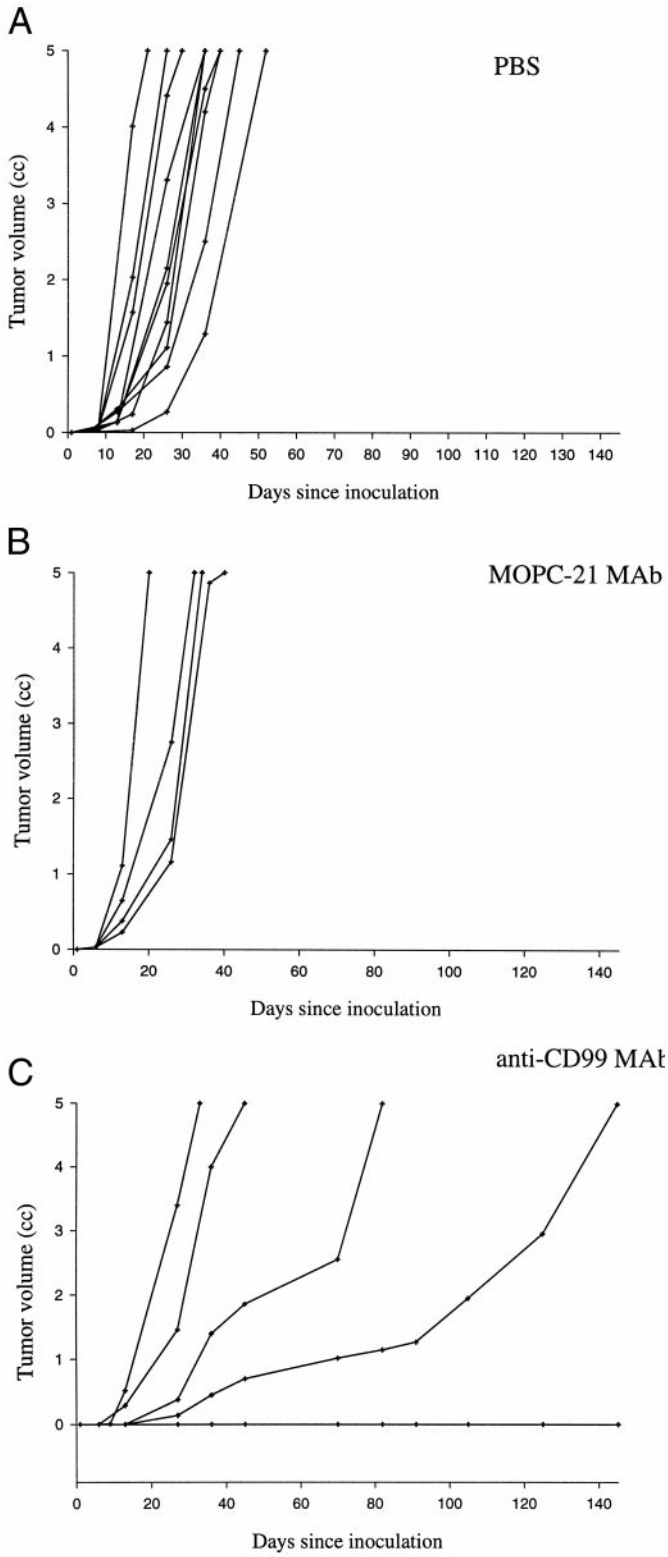

Fig. 6. Treatment of athymic mice with anti-CD99 MAb 0662 (40 μg/injection; eight injections) decreases the growth ability of 6647 cells. The *in vivo* growth curves of 6647 tumors in control (*A*), in MOPC21- treated (*B*), and in anti-CD99-treated (*C*) groups are shown. Each *line* corresponds to a single animal.

DISCUSSION

In this report, we first demonstrated that CD99 may be used as an immunotherapeutic tool for the treatment of EFT patients. In fact, engagement of CD99 induced a significant *in vitro* and *in vivo* inhibition of EFT growth by delivering an apoptotic signal and reducing the malignant potential of these cells. The *in vitro* growth inhibition of EFT cells induced by anti-CD99 MAb treatment ap-

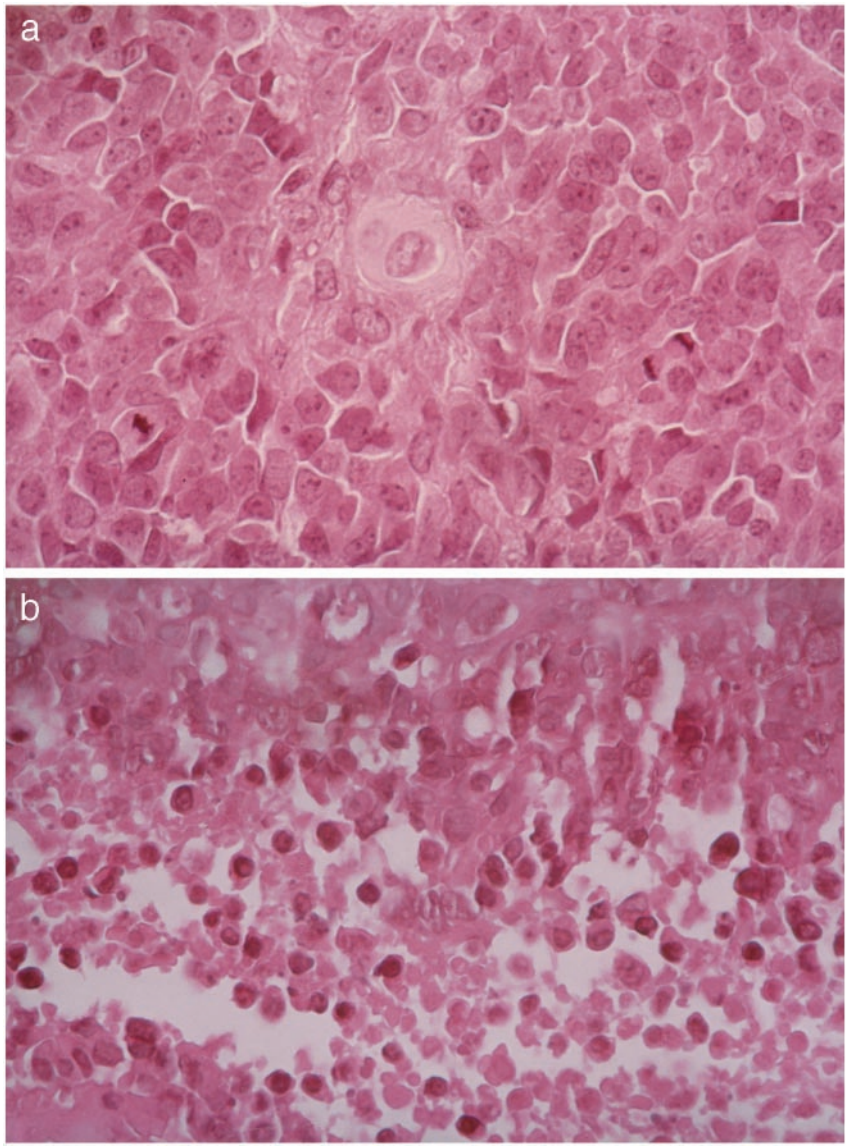

Fig. 7. Histological features of 6647 xenografts. *a*, untreated tumors show the typical monomorphous characteristics of EFT with some mitotic figures. *b*, 0662 MAb-treated tumors show the presence of apoptotic nuclei, featuring nuclear condensation and apoptotic body formation at the periphery of the lesion.

peared to be mainly attributable to the induction of massive apoptosis without any significant influence on the cell cycle distribution. CD99-induced apoptosis has already been described in thymocytes (18) and in some EFT cell lines (23). The analysis of the mechanisms underlying the apoptotic process in these cells suggested that apoptosis through CD99 molecules was devoid of prominent internucleosomal DNA fragmentation and did not involve the Fas pathway. Previous studies (18, 23) have suggested that CD99 can trigger a unique effective pathway involving caspase activation, chromatin condensation, and nucleus fragmentation without activation of internucleosomal endonucleases. In particular, the apoptotic process induced by CD99 engagement appears to be mainly attributable to a disruption of mitochondrial membrane functions, through the opening of the mitochondrial pores and the consequent $\Delta\psi m$ dissipation (23). Although a complete clarification of the CD99-induced death signaling certainly requires further investigations, our results confirm that CD99 may act as a functional protein in EFT cells by delivering an apoptotic signal. Differently from Sohn *et al.* (23), who have proposed that engagement of CD99 can trigger apoptosis only in the undifferentiated variants of EFT, we found that the ability of CD99 to induce growth inhibition through an apoptotic stimulus is strictly dependent on the level of expression of CD99, requiring the presence of a sufficient number of these molecules on the cell surface of EFT cells but being substantially independent from their neural differentiation phenotype. In addition to the effects on the *in vitro* cell growth, we found that CD99 cross-linking strongly impairs the ability of EFT cells to form colonies in soft agar and to produce tumors in nude mice. Whether these effects are the consequence of the massive induction of apoptosis after CD99 engagement or represent a specific impairment of the transformation processes in EFT cells need further investigation. However, the net result of anti-CD99 MAb treatment is a reduction of the growth ability and the malignant potential of EFT cells, further supporting the potential therapeutic value of CD99 as a specific target for innovative treatment of EFT patients. From a clinical point of view, to be of significant therapeutic value, MAbs against CD99 should be effectively combined with chemotherapeutic drugs. Most anticancer agents kill cancer cells by inhibiting cell cycle and/or inducing apoptosis (29–31). Therefore, chemotherapy- and CD99-induced EFT cell death may involve a common cytotoxic pathway that might be augmented by combination regimens. We found that anti-CD99 MAb potentiate the antitumor activity of doxorubicin and vincristin, two leader drugs in anti-EFT chemotherapy (6), in combined *in vitro* treatments. Taken together, these results provide a novel therapeutic approach that might have application in the therapy of EFT patients. Although a number of

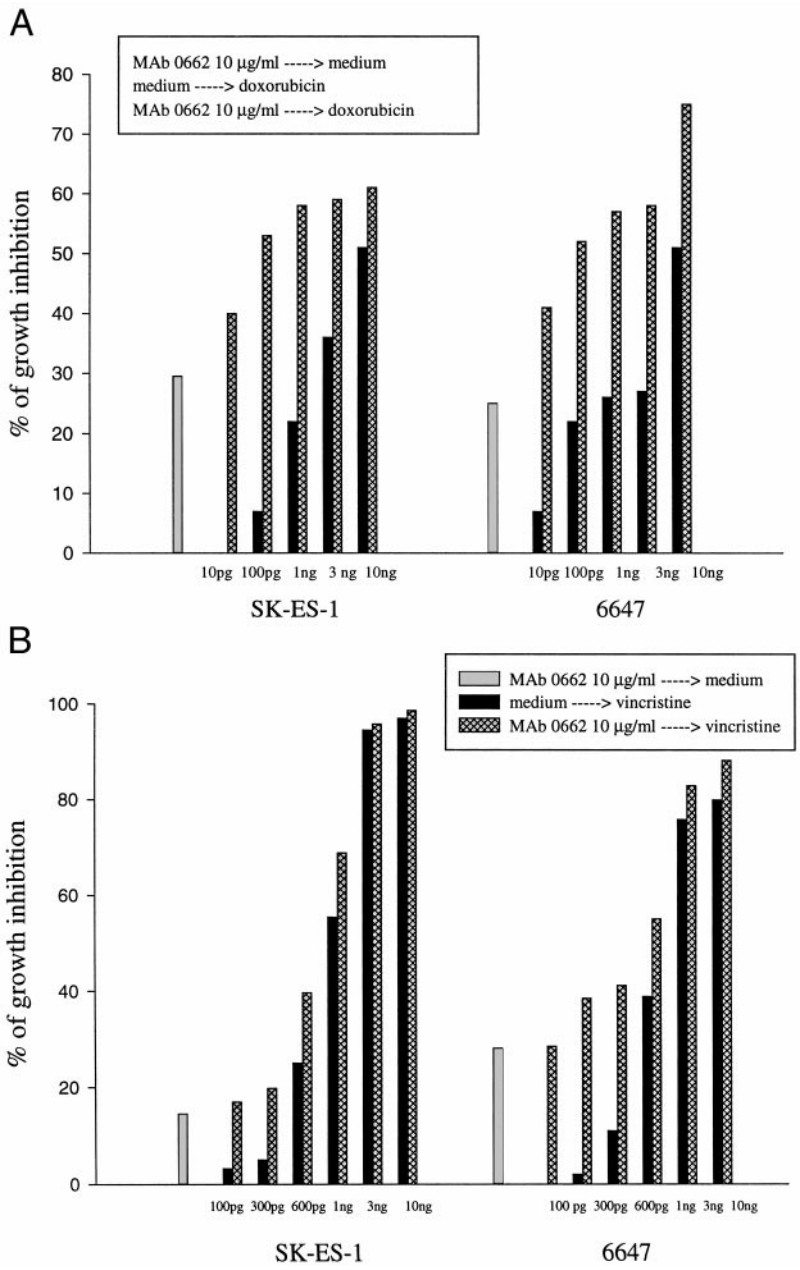

Fig. 8. Additive cytotoxicity of doxorubicin (*A*) or vincristine (*B*) in combination with 0662 MAb on two EFT cell lines after sequential treatments. EFT cells were treated with or without 0662 MAb (10 μg/ml) on the first day after cell seeding for a total of 12 h. Cells were then continuously exposed to different concentrations of chemotherapeutic agents for an additional 72 h.

significant obstacles have slowed the successful therapeutic application of MAbs (32), a series of Phase I and II clinical trials have been conducted in recent years to determine the safety and pharmacology of MAbs alone or in combination with chemotherapy, and two MAbs have been approved for the treatment of cancer (33, 34), indicating that MAbs are now part of the anticancer armamentarium. Of course, in the case of CD99 MAbs, their adequate selectivity for EFS application should be first analyzed, because the usefulness of CD99-targeted treatment of EFS patients could be limited by toxicity of this treatment on hematopoietic cells and particularly T lymphocytes.

In addition to its ability to deliver an apoptotic signal, CD99 cross-linking induced homotypic adhesion in EFT cells. Enhancement of cell-to-cell cohesive forces may reduce tumor cell motility, contributing to the immobilization of tumor cells, and in turn, to the inhibition of early events of the metastatic process (35). In lymphocytes, CD99 was demonstrated to play a role in their homotypic aggregation via the leukocyte function antigen-1/intercellular adhesion molecule-1 pathway (17). Enhancement of the expression level of several proteins, including MHC antigens, leukocyte function antigen-1, CD25, CD69, and CD40L after CD99 engagement has been observed in hematopoietic cells (17, 19, 20). At least for MHC molecules, it was clearly demonstrated that this increase was the result of an accelerated mobilization of molecules stored in cytosolic compartments rather than of increased RNA and protein synthesis (19). Recent studies have suggested that the activity of CD99 may be linked to the organization of the cytoskeleton and/or the activation of cytoskeletal components, likely through the Rac-Rho signaling pathway, thereby inducing accelerated mobilization of specific proteins (22). In particular, inhibition of the Rac-Rho pathway, which is known to play a role in the prevention of apoptosis as well as in the control of cell morphology, cell aggregation, and cytokinesis (36, 37), has been found to render lymphocytes insensitive to anti-CD99 antibody-triggered homotypic aggregation (22). These results, therefore, indicate that the Rac-Rho pathway functions downstream to CD99. This proc-

ess could also be involved in determining the increased cell-to-cell adhesion of EFT cells. Although the molecular mechanisms by which CD99 ligation causes these effects remains largely unknown, structural studies have identified in the region recognized by 0662 MAb (residues 66–74) and particularly in the phenylalanine residue (position 68), critical sites for mediating CD99-induced biological process (18). Additional studies are in progress in our laboratories to contribute to elucidate the signaling events resulting from CD99 engagement.

In conclusion, our data indicate that CD99 may play a role in different crucial processes of EFT cell biology, such as cell growth and transformation. These findings may have two relevant implications. From a clinical point of view, the demonstration that CD99 engagement significantly inhibits the *in vitro* and *in vivo* growth ability of EFT cells and that anti-CD99 MAb may be advantageously used in association with conventional chemotherapy opens new perspectives in the treatment of EFT. From a biological point of view, our results raise new questions on the function of this molecule. In fact, together with previous studies on hematopoietic (22, 38) and prostate carcinoma cells (39), our data further support the view of CD99 as a rather primitive marker associated, in its unbound form, with a poorer differentiation and a higher malignant potential. On the contrary, triggering of CD99 with specific MAbs induces cell-to-cell adhesion and cell death in immature thymocytes (16–18) and in EFT cells (23), cell proliferation in mature thymocytes (21), transport of transmembrane proteins (19, 20), and loss of malignancy of EFT cells. Therefore, CD99 appears to be an intriguing molecule, with multiple and controversial functions, the mechanisms of action of which are still poorly understood and certainly deserve further investigation.

REFERENCES

1. Campanacci, M. Ewing's sarcoma, primitive neuroectodermal tumor (PNET). *In:* M. Campanacci (ed.), Bone and soft tissue tumors, Ed. 2, pp. 653–682. New York: Springer-Verlag, 1999.
2. Delattre, O., Zucman, J., Melot, T., Garau, X. S., Zucker, J. M., Lenoir, G. M., Ambros, P. F., Sheer, D., Turc-Carel, C., Triche, T. J., Aurias, A., and Thomas, G. The Ewing family of tumors: a subgroup of small-round-cell tumors defined by specific chimeric transcripts. N. Engl. J. Med., *331:* 294–299, 1994.
3. Ambros, I. M., Ambros, P. F., Strehl, S., Kovar, H., Gadner, H., and Salzer Kuntschik, M. MIC2 is a specific marker for Ewing's sarcoma and peripheral primitive neuroectodermal tumors. Evidence for a common histogenesis of Ewing's sarcoma and peripheral primitive neuroectodermal tumors from MIC2 expression and specific chromosome aberration. Cancer (Phila.), *67:* 1886–1893, 1991.
4. Kovar, H., Dworzak, M., Strehl, S., Schnell, E., Ambros, I. M., Ambros, P. F., and Gadner, H. Overexpression of the pseudoautosomal gene *MIC2* in Ewing's sarcoma and peripheral primitive neuroectodermal tumor. Oncogene, *45:* 1067–1070, 1990.
5. Bacci, G., Toni, A., Avella, M., Manfrini, M., Sudanese, A., Ciaroni, D., Boriani, S., Emiliani, E., and Campanacci, M. Long-term results in 144 localized Ewing's sarcoma patients treated with combined therapy. Cancer (Phila.), *63:* 1477–1486, 1988.
6. Bacci, G., Picci, P., Ferrari, S., Mercuri, M., Brach del Prever, A., Rosito, P., Barbieri, E., Tienghi, A., and Forni, C. Neoadjuvant chemotherapy for Ewing's sarcoma of bone. No benefit observed after adding iphosphamide and etoposide to vincristine, actinomycin, cyclophosphamide, and doxorubicin in the maintenance phase. Results of two sequential studies. Cancer (Phila.), *6:* 1174–1183, 1998.
7. Craft, A., Cotterill, S., Malcolm, A., Spooner, D., Grimer, R., Souhami, R., Imeson, J., and Lewis, I. Ifosfamide-containing chemotherapy in Ewing's sarcoma: the Second United Kingdom Children's Cancer Study Group and the Medical Research Council Ewing's Tumor Study. J. Clin. Oncol., *16:* 3628–3633, 1998.
8. Horowitz, M. E., Kinsella, T. J., Wexler, L. H., Belasco, J., Triche, T., Tsokos, M., Steinberg, S. M., McClure, L., Longo, D. L., Steis, R. G., Glatstein, E., Pizzo, P. A., and Miser, J. S. Total-body irradiation and autologous bone marrow transplant in the treatment of high-risk Ewing's sarcoma and rhabdomyosarcoma. J. Clin. Oncol., *11:* 1911–1918, 1993.
9. Paulussen, M., Ahrens, S., Craft, A. W., Dunst, J., Frohlich, B., Jabar, S., Rube, C., Winkelmann, W., Wissing, S., Zoubek, A., and Jurgens, H. Ewing's tumors with primary lung metastases: survival analysis of 114 (European Intergroup) Cooperative Ewing's Sarcoma Studies patients. J. Clin. Oncol., *16:* 3044–3052, 1998.
10. Scotlandi, K., Benini, S., Sarti, M., Lollini, P-L., Maurici, D., Picci, P., Manara, M. C., and Baldini, N. Insulin-like growth factor I receptor-mediated circuit in Ewing's sarcoma/peripheral neuroectodermal tumor: a possible therapeutic target. Cancer Res., *56:* 4570–4574, 1996.
11. Scotlandi, K., Benini, S., Nanni, P., Lollini, P-L., Nicoletti, G., Landuzzi, L., Serra, M., Manara, M. C., Picci, P., and Baldini, N. Blockage of insulin-like growth factor-I receptor inhibits the growth of Ewing's sarcoma in athymic mice. Cancer Res., *58:* 4127–4131, 1998.
12. Goodfellow, P. J., Darling, S. M., Thomas, N. S., and Goodfellow, P. N. A pseudoautosomal gene in man. Science (Washington DC), *234:* 740–743, 1986.
13. Banting, G. S., Pym B., Darling, S. M., and Goodfellow, P. N. The MIC2 gene product: epitope mapping and structural prediction analysis define an integral membrane protein. Mol. Immunol., *26:* 181–188, 1989.
14. Gelin, C., Aubrit, F., Phalipon, A., Raynal, B., Cole, S., Kaczorek, M., and Bernard, A. The E2 antigen, a 32 kDaglycoprotein involved in T cell adhesion process, is the MIC2 gene product. EMBO J., *8:* 3253–3259, 1989.
15. Bernard, A., Aubrit, F., Raynal, B., Pham, D., and Boumsell, L. A T cell surface molecule different from CD2 is involved in spontaneous rosette formation with erythrocytes. J. Immunol., *140:* 1802–1807, 1988.
16. Bernard, G., Zoccola, D., Deckert, M., Breittmayer, J-P., Aussel, C., and Bernard, A. The E2 molecule (CD99) specifically triggers homotypic aggregation of $CD4^+CD8^+$ thymocytes. J. Immunol., *154:* 26–32, 1995.
17. Hahn, J-H., Kim, M. K., Choi, E. Y., Kim, S. H. Sohn, H. W., Ham, D. I., Chung D. H., Kim, T. J. Lee, W. J., Park, C. K., Ree, H. J., and Park, S. H. CD99 (*MIC2*) regulates the LFA-1/ICAM-1-mediated adhesion of lymphocytes, and its gene encodes both positive and negative regulators of cellular adhesion. J. Immunol., *159:* 2250–2258, 1997.
18. Bernard, G., Breittmayer, J-P., de Matteis, M., Trampont, P., Hofman, P., Senik, A., and Bernard, A. Apoptosis of immature thymocytes mediated by E2/CD99. J. Immunol., *158:* 2543–2550, 1997.
19. Choi, E. Y., Park, W. S., Jung, K. C., Kim, S. H., Kim, Y. Y., Lee, W. J., and Park, S. H. Engagement of CD99 induces up-regulation of TCR and MHC class I and II molecules on the surface of human thymocytes. J. Immunol., *161:* 749–754, 1998.
20. Wingett, D., Forcier, K., and Nielson, C. P. A role for CD99 in T cell activation. Cell. Immunol., *193:* 17–23, 1999.
21. Waclavicek, M., Majdic, O., Stulnig, T., Berger, M., Sunder-Plassmann, R., Zlabinger, G. J., Baumruker, T., Stöckl, J., Ebner, C., Knapp, W., and Pickl, W. F. CD99 engagement on human peripheral blood T cells results in TCR/CD3-dependent cellular activation and allows for Th1-restricted cytokine production. J. Immunol., *161:* 4671–4678, 1998.
22. Kim, S. H., Choi, E. Y., Shin, Y. K., Kim, T. J., Chung, D. H., Chang, S. I., Kim, N. K., and Park, S. H. Generation of cells with Hodgkin's and Reed-Sternberg phenotype through downregulation of CD99 (*Mic2*). Blood, *92:* 4287–4295, 1998.
23. Sohn, H. W., Choi, E. Y., Kim, S. H., Lee, I., Chung, D. H., Sung, U. A., Hwang, D. H., Cho, S. S., Jun, B. H., Jang, J. J., Chi, J. G., and Park, S. H. Engagement of CD99 induces apoptosis through a calcineurin-independent pathway in Ewing's sarcoma cells. Am. J. Pathol., *153:* 1937–1945, 1998.
24. Gelin, C., Zilber, M-T., Jovanovich, D., and Boumsell, L. The E2/MIC2 molecule is defined by cluster of differentiation CD99. *In:* S. F. Schlossman, L. Boumsell, W. Gilks, J. M. Harlan, T. Kishimoto, C. Morimoto, J. Ritz, S. Shaw, R. Silverstein, T. Springer, T. F. Tedder, and R. F. Todd (eds.), Leucocyte Typing V. White Cell Differentiation Antigens. Proceedings of the Fifth International Workshop and Conference, pp. 283–285. Oxford: Oxford University Press, 1995.
25. Scotlandi, K., Serra, M., Nicoletti, G., Vaccari, M., Manara, M. C., Nini, G., Landuzzi, L., Colacci, A., Bacci, G., Bertoni, F., Picci, P., Campanacci, M., and Baldini, N. Multidrug resistance and malignancy in human ostedsarcoma. Cancer Res., *56:* 2434–2439, 1996.
26. Koopman, G., Reutelingsperger, C. P., Kuijten, G. A., Keehnen, R. M., Pals, S. T., and van Oers, M. H. Annexin V for flow cytometric detection of phosphatidylserine expression on B cells undergoing apoptosis. Blood, *84:* 1415–1420, 1994.
27. Martin, S. J., Reutelingsperger, C. P., McGahon, A. J., Rader, J. A., van Schie, R. C., LaFace, D. M., and Green, D. R. Early redistribution of plasma membrane phosphatidylserine is a general feature of apoptosis regardless of the initiating stimulus: inhibition of overexpression of Bcl-2 and Abl. J. Exp. Med., *182:* 1545–1556, 1995.
28. Schulze-Osthoff, K., Ferrari, D., Los, M., Wesselborg, S., and Peter, M. E. Apoptosis signaling by death receptors. Eur. J. Biochem., *254:* 439–459, 1998.
29. Eastman, A. Activation of programmed cell death by anticancer agents: cisplatin as a model system. Cancer Cells, *2:* 275–280, 1990.
30. Friesen, C., Herr, I., Krammer, P. H., and Debatin, K-M. Involvement of the CD95 (APO-1/Fas) receptor/ligand system in drug-induced apoptosis in leukemia cells. Nat. Med., *2:* 574–577, 1996.
31. Waldman, T. Zhang, Y., Dillehay, L., Yu, J., Kinzler, K., Vogelstein, B., and Williams, J. Cell-cycle arrest *versus* cell death in cancer therapy. Nat. Med., *3:* 1034–1036, 1997.
32. Junghans, R. P., Sgouros, G., and Scheinberg, D. A. Antibody-based immunotherapies for Cancer. *In:* B. A. Chabner and D. L. Longo (eds.), Cancer Chemotherapy and Biotherapy. Principles and Practice, pp. 655–689. Philadelphia: Lippincott-Raven, 1996.
33. Baselga, J., and Mendelsohn, J. Receptor blockade with monoclonal antibodies as anti-cancer therapy. Pharmacol. Ther., *64:* 127–154, 1994.
34. Dillman, R. O. Unconjugated monoclonal antibodies for the treatment of hematologic and solid malignances. American Society of Clinical Oncology: Educational Book, pp. 461–468, 1999.
35. Fidler, I. J. Molecular biology of cancer: invasion and metastasis. *In:* V. T. De Vita, S. Hellman, and S. A. Rosenberg (eds.), Cancer: Principles and Practice of Oncology, Ed. 5, pp. 135–152. Philadephia: Lippincott-Raven Publishers, 1997.
36. Takai, Y., Sasaki, T., Tanaka, K., and Nakanishi, H. Rho as a regulator of the cytoskeleton. Trends Biochem. Sci., *20:* 227–231, 1995.
37. Tsubakimoto, K., Matsumoto, K., Abe, H., Ishii, J., Amano, M., Kaibuchi, K., and Endo, T. Small GTPase RhoD suppresses cell migration and cytokinesis. Oncogene, *18:* 2431–2440, 1999.
38. Dworzak, M. N., Fritsch, G., Fleischer, C., Printz, D., Fröschl, G., Buchinger, P., Mann, G., and Gadner, H. CD99 (MIC2) expression in paediatric B-lineage leukemia/lymphoma reflects maturation-associated patterns of normal B-lymphopoiesis. Br. J. Haematol., *105:* 690–695, 1999.
39. Shen J., Zhau, H. E., Hursting, S. D., and Chung, L. W. Androgen regulation of the human pseudoautosomal gene *MIC2*, a potential marker for prostate cancer. Mol. Carcinog., *23:* 13–19, 1998.

CD99 Engagement: An Effective Therapeutic Strategy for Ewing Tumors

Katia Scotlandi, Nicola Baldini, Vanessa Cerisano, et al.

Cancer Res 2000;60:5134-5142.